

## Research Article



Check for updates

OPEN

# Marine Actinobacteria amo.128 Isolated from Seribu Island: Antibacterial, Antibiofilm and Molecular Docking as Quorum Sensing Inhibitors

**Heru Agus Cahyanto<sup>1</sup>, Rofiq Sunaryanto<sup>2\*</sup>, Ema Damayanti<sup>2</sup>, Mustofa<sup>3</sup>**<sup>1</sup>Research Center for Pharmaceutical Ingredients and Traditional Medicine, National Research and Innovation Agency, Cibinong, Bogor 16911, Indonesia<sup>2</sup>Research Center for Food Technology and Processing, BRIN, National Research and Innovation Agency, Gunungkidul, Yogyakarta, Indonesia<sup>3</sup>Department of Pharmacology and Therapy, Faculty of Medicine, Public Health and Nursing, Gajah Mada University, Yogyakarta, Indonesia**ARTICLE INFO****Article history:**

Received December 27, 2024

Received in revised form March 21, 2025

Accepted April 9, 2025

**KEYWORDS:**antibacterial,  
antibiofilm,  
actinomycete,  
quorum-sensing inhibitor

Copyright (c) 2025@ author(s).

**ABSTRACT**

The prevalence of antibiotic-resistant bacteria is increasing every year in Indonesia. This resistance occurs in several antimicrobial categories. A contributing factor to microbial resistance is the capacity of microbes to develop biofilms. Amo.128 is an actinomycete from the Laboratory Biotechnology, BRIN Serpong collection, which is expected to have both antimicrobial and antibiofilm activity. This study aimed to identify amo.128 macroscopically, microscopically, and molecularly; to determine the antibacterial and antibiofilm activity; to identify secondary metabolites; and to understand the mechanism of quorum sensing inhibition by *in silico* with proteins targeting *SdiA* and *AgrA*. Based on macroscopic and microscopic observations, the amo.128 isolate belongs to the genus *Streptomyces*. Phylogenetic analysis of the amo.128 isolate is 100% similar to *Streptomyces parvus* strain NBRC 14599. The amo.128 metabolite contains several compounds, including N-acetyltyramine, cyclophenylalanylprolyl/cFP, and the pyrrole-pyrazine group. The MIC/MBC/MIC<sub>50</sub> value of the amo.128 metabolite against *Staphylococcus aureus* is 25/50/28.48 ppm, while for *Escherichia coli* it is 100/200/49.38 ppm. The amo.128 metabolite reduced biofilms formed by *S. aureus* and *E. coli* with BRC<sub>50</sub> values of 62.07 ppm and 60.44 ppm, respectively. The amo.128 metabolite compound, cyclophenylalanylprolyl/cFP, has potential activity as a quorum-sensing inhibitor.

## 1. Introduction

The prevalence of antibiotic-resistant bacteria is increasing every year in Indonesia, driven by the overuse and misuse of antimicrobial agents (Gach *et al.* 2024). Bacteria become resistant not only to one type of antimicrobial but also to several categories known as Multi-Drug Resistance/MDR (Magiorakos *et al.* 2012). This has become a serious problem because resistant bacteria caused many deaths in Indonesia through infectious diseases (WHO 2024). Infectious diseases

are widely associated with pathogens that form biofilms (Gach *et al.* 2024). This has prompted the exploration of new antimicrobials or antibiofilms that are more sensitive to pathogens.

*Staphylococcus aureus* and *Escherichia coli* are widely associated with their ability to form biofilm (Gunathilaka *et al.* 2024; Wu *et al.* 2024). Biofilm is a complex structure of microbes contained in a matrix called extracellular polymeric substance/EPS, which is composed of polysaccharides, lipopolysaccharides, lipids, proteins, and eDNA (Karygianni *et al.* 2020). Biofilm formation begins with a process of aggregation and attachment, followed by growth and accumulation,

---

<sup>\*</sup> Corresponding Author

E-mail Address: rofi001@brin.go.id

which ultimately occurs in deaggregation and dispersal (Sauer *et al.* 2022).

Biofilm formation is mediated by a system known as quorum sensing. Quorum sensing is a mechanism to regulate gene expression depending on cell density (Karygianni *et al.* 2020). Gram-positive bacteria use acyl homoserine lacton/AHL, while negative bacteria use AIP to communicate with each other. Gene activation by quorum sensing is responsible for the expression of virulence factors, enzyme secretion, synthesis of antimicrobial substances, and biofilm formation (Suresh *et al.* 2021). Biofilm will increase microbial resistance to antimicrobial compared to planktonic cells (Pompilio *et al.* 2023; Gunathilaka *et al.* 2024).

The discovery of new drugs is necessary to overcome microbial resistance, which has caused many deaths (WHO 2017). Several studies have been carried out to find antimicrobial and antibiofilm compounds, but they are still lacking. There are still opportunities for the exploration and development of antimicrobial sources. Actinomycetes have a great opportunity to be explored to obtain antibiofilm and antibiofilm antimicrobial compounds (Miller *et al.* 2022).

Actinomycetes are gram-positive, anaerobic, or facultative bacteria living as saprophytes or decomposers. Actinomycetes has activity as an antibacterial, antifungal, antiparasitic, anti-inflammatory, antioxidant, anticancer, and also as a immunomodulator (Wang *et al.* 2017; El Karkouri *et al.* 2019; Sarika *et al.* 2021). Its metabolites include polyketide compounds, alkaloids, steroids, fatty acids, peptides, and terpene compounds. It also contains enzymes such as amylase, cellulase, lipase, and proteases that can degrade polysaccharides and proteins in biofilms (Asnani *et al.* 2016).

The isolate actinomycetes amo.128 is an isolate that is symbiotic with the marine snail (*Littorina scabra*) obtained from Seribu Island. Amo.128 isolate needs to be re-identified to ensure the microbe's identity/type and characteristics that will be used to produce antibacterial and antibiofilm test compounds. We macroscopically, microscopically, and molecularly identify the amo.128 isolate from Seribu Island, Jakarta, and then determine the activity of metabolite of amo.128 as the antibacterial, antibiofilm, and anti-quorum sensing or as a quorum-sensing inhibitor.

## 2. Materials and Methods

### 2.1. Biological Material

Actinomycete amo.128 was used in this experiment and isolated from the marine snail (*Littorina scabra*)

obtained from Seribu Island, North Jakarta. Actinomycete amo.128 is stored in glycerol stock at the Biotechnology Laboratory BRIN Serpong. Amo.128 was grown again on the International *Streptomyces* Project-2 (ISP2) medium.

### 2.2. Fermentation and Extraction

Fermentation and extraction were carried out according to Sunaryanto (Sunaryanto *et al.* 2009). The isolate was cultivated on 50 ml of Yeast Extract Malt Extract (YEME) broth vegetative mediums (peptone, yeast extract, malt extract, glucose/5:3:3:10) in Erlenmeyer 250 ml at 30°C, shaker at 150 rpm for 2 days, then transferred to 250 ml fermentative mediums (peptone, yeast extract, Fe(III) citrate hydrate, glucose/5:1:0,3:5) at 1,000 ml flash and incubated at 30°C with a shaker at 150 rpm for 5 days. Ethyl acetate (1:1) was added in a bottle flash and homogenized in a shaker. The supernatant was separated and steamed in a rotary evaporator. A little absolute methanol was added and put into a concentrator to obtain a dry extract.

### 2.3. Macroscopic, Microscopic Characterization

Macroscopic and microscopic characterization was performed to examine the morphology of the isolate, which was cultivated on ISP2 media. Microscopic characterization was done using a microscope, while macroscopic characterization was done using a microscope and looking at objects directly. Observations include the presence or absence of aerial mycelium, spore shape, shape colony, and colony color.

### 2.4. Molecular Characterization

DNA extraction and amplification of 16S rRNA sequences according to InstageneTM protocol. The primers 8F (5'-AGA, GTT, TCC, TGG, CTC, AG-3') and 1492R (5'-GGA TAC, CTT, GTT, ACG, ACT, T-3') were used for amplification. Amplification was carried out at a volume of 10  $\mu$ M. The programs were as follows: pre-denaturation at 96°C for 30 seconds, denaturation at 96°C for 10 seconds, annealing at 56°C for 30 seconds, extension at 72°C for 30 seconds, and final extension at 72°C for 5 minutes. The results were followed by electrophoresis on 1% agarose gel with ethidium bromide staining. Sequencing used the same primers, namely 8F and 1492R. Identification of amo.128 using the 16S rRNA gene and alignment of forward and reverse nucleotide sequences using BioEdit software. Phylogenetic distance analysis using MEGA11 software.

## 2.5. Liquid Chromatography-High Resolution and Mass Spectrometry (LC-HRMS) and Fourier Transform Infra-Red (FTIR) Spectroscopy Analysis

The method LCHRMS is based on Windarsih (Windarsih *et al.* 2022) using a Thermo Scientific™ Accucore™ Phenyl-Hexyl column 100 mm × 2.1 mm ID × 2.6 µm. The mobile phases use 0.1% formic acid (A) and 0.1% formic acid (B). MS-grade methanol gradient elution system: 0-16 min (5-90% B); 4 min (90% B); 25 min (5% B) with a flow rate of 0.3 ml/min. The column temperature was 40°C, and the injection volume was 3 µL. Sheath, auxiliary, and sweep using Nitrogen gas were set at 32, 8, and 4 arbitrary units (AU). The mass spectrometer system parameter was set as follows: the spray voltage was 3.30 kV, the capillary temperature was 320°C, and the auxiliary gas heater temperature was set at 30°C. The m/z range was performed at 66.7–1000, and the resolution used was 70,000 for full MS and 17,500 for dd-MS2. Results were analyzed using XCalibur 4.4 software (Thermo Scientific, Bremen, Germany).

FTIR analysis using the Attenuated Total Reflectance (ATR) method allows for sample examination without the pelletization process involving KBr.

## 2.6. Antibacterial and Antibiofilm Assay

The antibacterial assay was performed using the microdilution assay (Setiawati 2021). 5 µL suspension of *S. aureus* and *E. coli* were inoculated in 5 ml of Mueller Hinton Broth (MHB) medium in a 15 ml Falcon tube and incubated for 24 hours. Dilution of the bacterial suspension was made at a concentration of  $1 \times 10^7$  CFU/ml by comparing it with the Mc. Farland standard. The amo.128 metabolite extract was prepared in eight levels of concentration (3.125-400 µg/ml in 1% of Dimethyl Sulfoxide (DMSO) as solvent) and re-diluted using MHB medium. Then, add 5 µL to eight levels of concentration of extract in a 96-well microplate and incubate at 37°C for 24 hours. Mark the clear well as a minimum inhibition concentration (MIC) and read optical density with a microplate reader at 540/600 nm to calculate inhibition.

$$\% \text{ Inhibition} = \frac{\text{OD average pathogen} - \text{OD average sample}}{\text{average patogen}} \times 100\%$$

Minimum Bactericidal Concentration (MBC) is calculated by scratching one loop inoculum per well on the agar medium. The minimal concentration at which no microbial growth is observed is called the MBC.

The antibiofilm test was performed using the crystal violet assay according to Nirwati with slight modifications (Nirwati *et al.* 2022). Planktonic cells were removed by washing with phosphate-buffered saline (PBS) solution three times after 24 h of incubation. Add 1% CV (Crystal violet) color and let sit for 15 minutes. Wash using sterile distilled water, then add 96% ethanol. Move it into a new microplate and read the optical density at a wavelength of 595 nm using a microplate reader.

$$\% \text{ Biofilm reduction} = \frac{\text{OD average pathogen} - \text{OD average sample}}{\text{average patogen}} \times 100\%$$

## 2.7. Scanning Electron Microscope (SEM)

Biofilms were observed using SEM according to the previous study with modifications (Nirwati *et al.* 2022). Biofilms were grown at 37°C for 24 hours on sterile coverslips in a 24-well microplate in the presence of inhibitory concentrations of isolate extract. The biofilm that was not exposed to the actinomycetes extract was used as a control. After incubation, the coverslip was washed twice with sterile PBS and dehydrated in an ethanol series (70% for 10 min, 95% for 10 min, and 100% for 20 min) and air-dried overnight. The coverslip was coated with Aurum and observed using SEM.

## 2.8. Molecular Docking

Molecular docking was done as a quorum-sensing inhibitor that uses protein targets 4LGW, 4G4K, and 3QP5. Ligan structure was downloaded from PubChem according to LC-HRMS results. Autodocktools 1.5.7 was used to separate and validate proteins from native ligands. Pymol and Autodock Vina were used for the docking process and visualization by Discovery Studio 2021.

## 2.9. Statistical Analysis

All the experiments were performed in triplicate, and data were provided as mean  $\pm$  SD. Data were performed in the percentage (%) of inhibition and analyzed using SPSS 2022. Linear regression analysis was used to determine the  $\text{MIC}_{50}$  and  $\text{BC}_{50}$  parameters.

## 2.10. Ethical Clearance

Ethical clearance was obtained from the Medical and Health Research Ethics Committee of the Faculty of Medicine, Public Health and Nursing, Universitas Gadjah Mada, Yogyakarta (ref. No. KE/KF/0994/EC/2024).

### 3. Results

#### 3.1. Yield of Extract

Fermentation was carried out to obtain secondary metabolites from amo.128. Amo.128 grows in a yellowish-colored fermentation medium, so a yellowish dry extract is formed when extracted and evaporated with ethyl acetate. The yield obtained was 0.0124 %.

#### 3.2. Morphology of amo.128

Actinomycetes amo.128 grown in ISP2 media, as seen in Figure 1, has a gray color (front view), irregular shape and size, and sandy surface.



Figure 1. Macroscopic characterization of amo.128 morphology growing on ISP2 agar

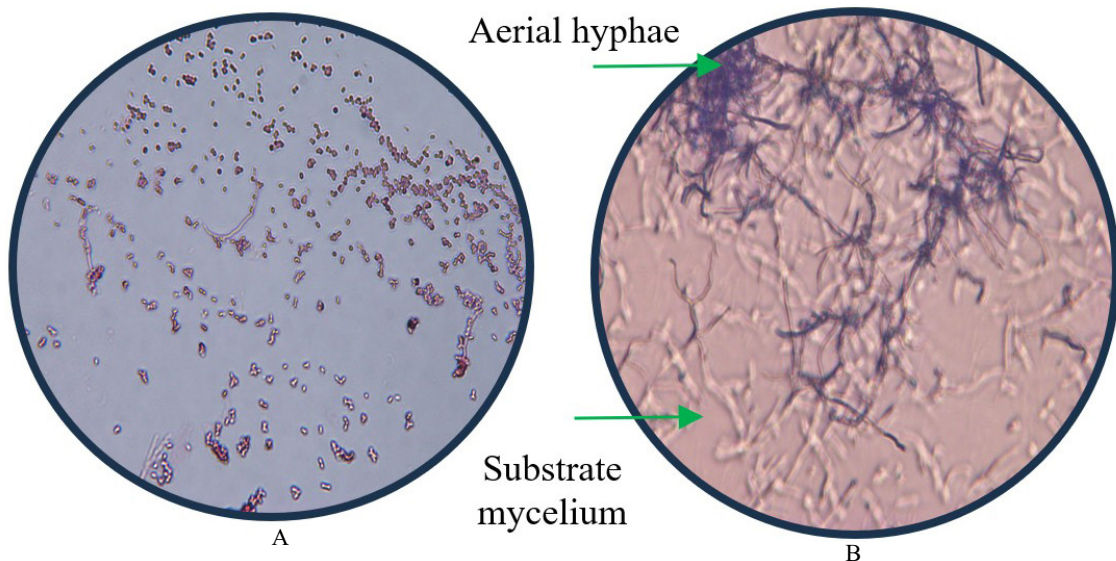


Figure 2. Macroscopic characterization with magnification 50X. (A) Amo.128 isolate with Gram staining, (B) Amo.128 isolate growing on ISP2 agar

Amo.128 appears as a single colony, distinctive purple after gram staining (Figure 2A). Hyphae are visible when grown on ISP2 agar media and viewed using a microscope (Figure 2B).

#### 3.3. 16S rRNA Gene Sequence Amplification Results and Phylogenetic Tree of Actinomycetes amo.128.

Figure 3 shows the electrophoresis results on 1% agarose gel of the PCR product. A single band with a length of 1500 bp was observed. Determination of the actinomycetes amo.128 species was performed at the species level by sequencing the 16S rRNA gene and BLAST-based on sequences obtained with the NCBI database. Figure 4 displays the phylogenetic position of Actinomycetes amo.128, which is 100% similar to *Streptomyces parvus* NBRC 14599.

#### 3.4. Metabolites Substances of amo.128

The results of the LC-HRMS identification of the ethyl acetate extract amo 128 are shown in Table 1. The chemical content obtained includes alkaloids, cyclic dipeptides, heterocyclic nitrogen, fatty acids, and phenol derivatives. The main compound contained in the ethyl acetate extract of actinomycetes amo.128 is alkaloids N-acetyltyramine.

#### 3.5. MIC, MBC, and MIC<sub>50</sub> values of amo.128

The antibacterial activity against gram-positive bacteria, specifically *S. aureus*, is more potent than that against gram-negative bacteria, *E. coli*. The MIC and MBC are illustrated in Figures 5 and 6. The

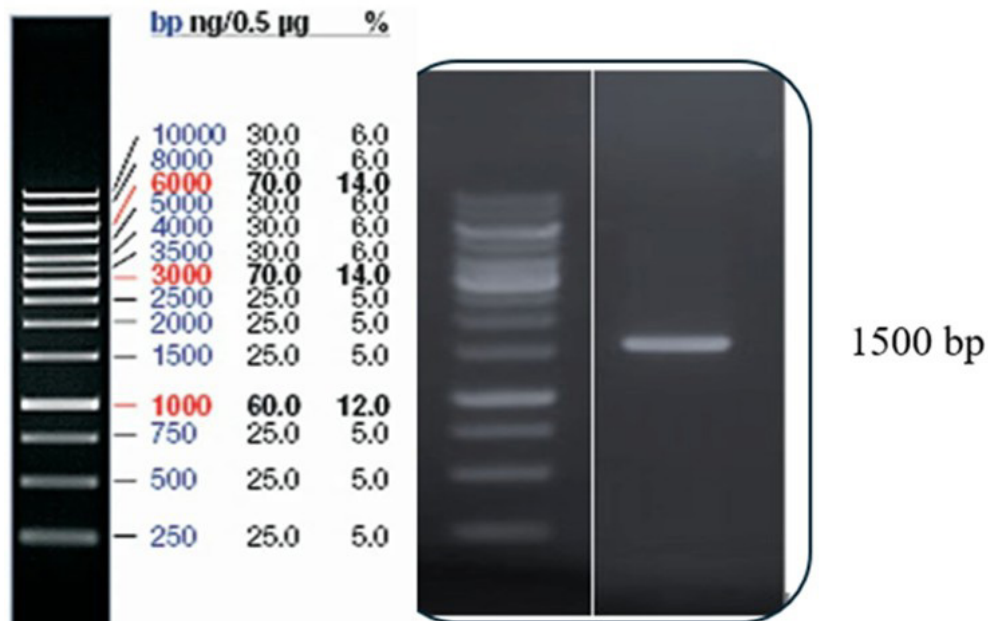


Figure 3. Agarose gel electrophoresis analysis of 16S rRNA genes amplified from amo.128 isolates. PCR-amplified products were run on 1% agarose gel

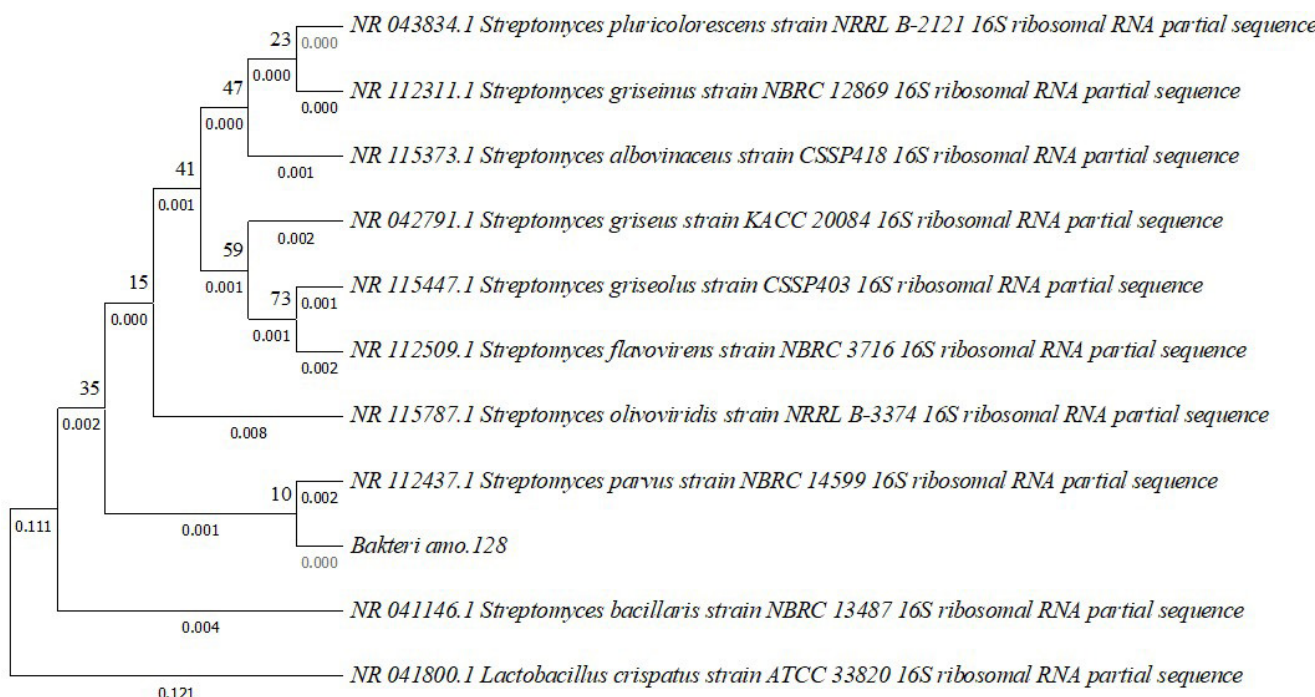


Figure 4. Phylogenetic trees based on the 16S rRNA sequences of amo.128 isolate were compared with the neighbor-joining method using the MEGA 11

Table 1. The main content of amo.128 metabolite compounds using LC-HRMS

Name	Group	Formula	RT (Min)	Activity	Anot source: cloud search	m/z best match	mz cloud	Relative abundance (%)
N-acetyl tyramine	Alkaloid	C <sub>10</sub> H <sub>13</sub> N O <sub>2</sub>	4.056	quorum sensing inhibitor/qsi (Reina et al. 2019)	Full match	Full match	Full match	16.66
cyclo(phenylalanylprolyl)	Cyclic dipeptide	C <sub>14</sub> H <sub>16</sub> N <sub>2</sub> O <sub>2</sub>	6.036	antibiofilm and quorum sensing inhibitor (Li et al. 2022)	Full match	Full match	Full match	7.97
3-(propane-2-yl)-octahydropyrrolo[1,2-a]pyrazine-1,4-dione	Heterocyclic nitrogen	C <sub>10</sub> H <sub>16</sub> N <sub>2</sub> O <sub>2</sub>	3.774	antibacterial, antivirus, antifungal, antitumor (Dehnavi et al. 2021)	Full match	Full match	Full match	4.02
3-[(4-hydroxyphenyl)methyl]-octahydropyrrolo[1,2-a]pyrazine-1,4-dione	Heterocyclic nitrogen	C <sub>14</sub> H <sub>16</sub> N <sub>2</sub> O <sub>3</sub>	3.815	antibacterial, antivirus, antifungal, antitumor (Dehnavi et al. 2021)	Full match	Full match	Full match	2.43
palmitoleic acid	Fatty acid	C <sub>16</sub> H <sub>30</sub> O <sub>2</sub>	14.601	antibacterial (Wang et al. 2022)	Full match	Full match	Full match	0.17
4-methoxycinnamic acid	Phenol-derivative	C <sub>10</sub> H <sub>10</sub> O <sub>3</sub>	15.0.	Antibacterial, antifungal, and anti-inflammatory (Wang et al. 2023)	Full match	Full match	Full match	0.11
Monoolein	Fatty acid	C <sub>21</sub> H <sub>40</sub> O <sub>4</sub>	17,759	antibacterial (Nitbani et al. 2020)	Full match	Full match	Full match	0.07

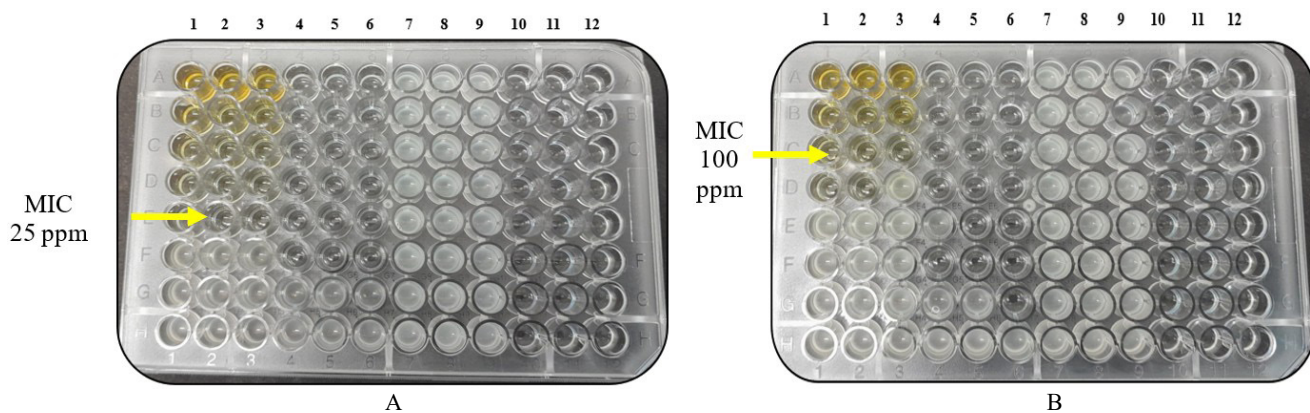


Figure 5. Microbroth dilution method using a 96-well microtiter plate to measure MIC metabolites amo.128 to (A) *S. aureus*. MIC metabolites amo.128 to (B) *E. coli*. Columns 1, 2, and 3 for metabolites amo.128. Columns 4, 5, and 6 are wells for ampicillin. Columns 7, 8, and 9 are wells for pathogen control, while columns 10, 11, and 12 were used for media control

MIC<sub>50</sub> value also confirms that the extract is stronger against gram-positive bacteria (Figure 7). However, the ability to reduce biofilm showed no difference (Figure 8).

### 3.6. Cell Morphology

Cell morphology was observed after treatment at MIC and MBC concentrations. Figures 9 and 10

depict bacteria (*S. aureus* and *E. coli*) given with ampicillin treatment, Figure 11 shows the control without treatment, and Figures 12 and 13 show the antibacterial activity of amo128 extract. The extract of Amo.128 shows antibacterial and antibiofilm properties; however, its effectiveness is still lower compared to ampicillin.

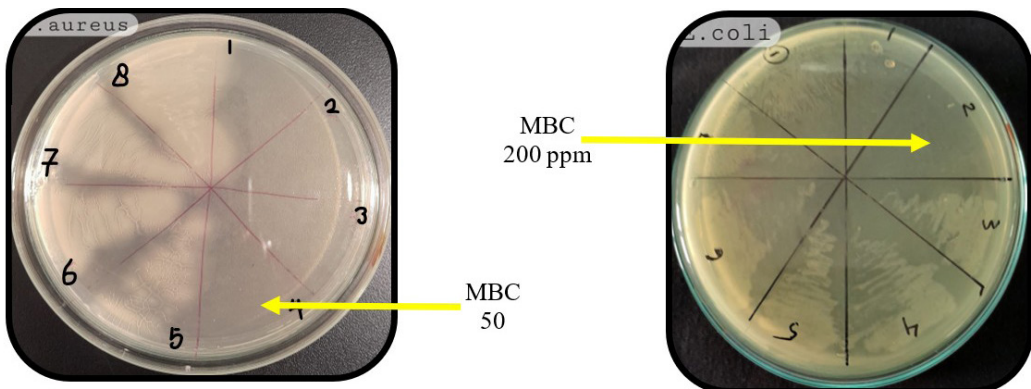


Figure 6. Determination of MBC of metabolites amo.128 through their cultures on MHA medium. MBC metabolites amo.128 to *S. aureus* is 50 ppm. MBC metabolites amo.128 to *E. coli* is 200 ppm

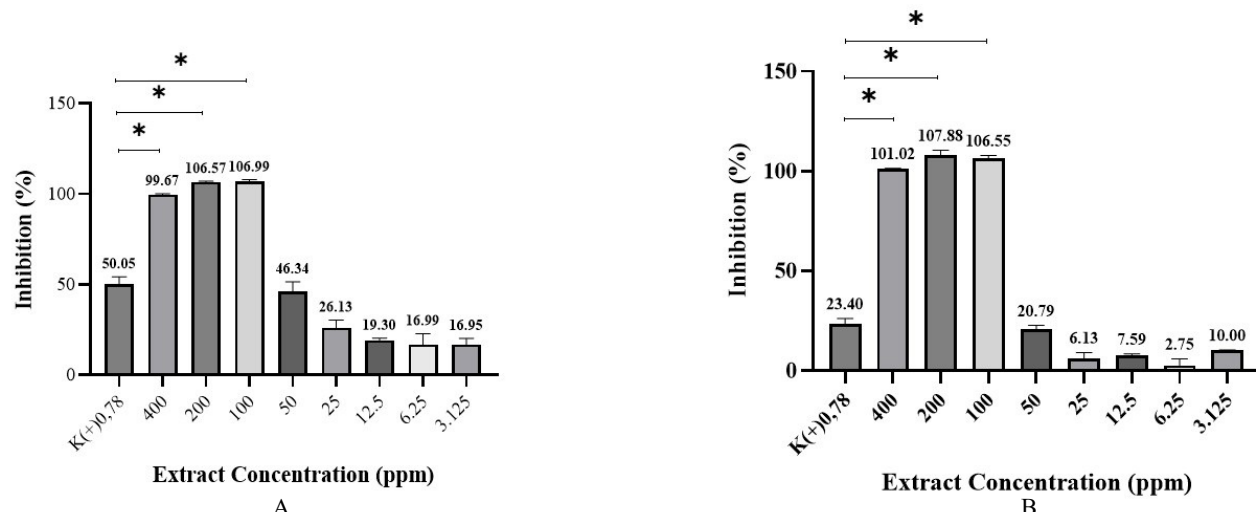


Figure 7. (A) Antibacterial activity metabolites amo.128 to *S. aureus*. MIC<sub>50</sub> is 28.48 ppm. (B) Antibacterial activity metabolites amo.128 actinomycetes to *E. coli*. MIC<sub>50</sub> is 49.38 ppm. Statistical analysis was performed using one-way ANOVA, followed by Tukey's post hoc test with a sig. level of p-value of <0.05

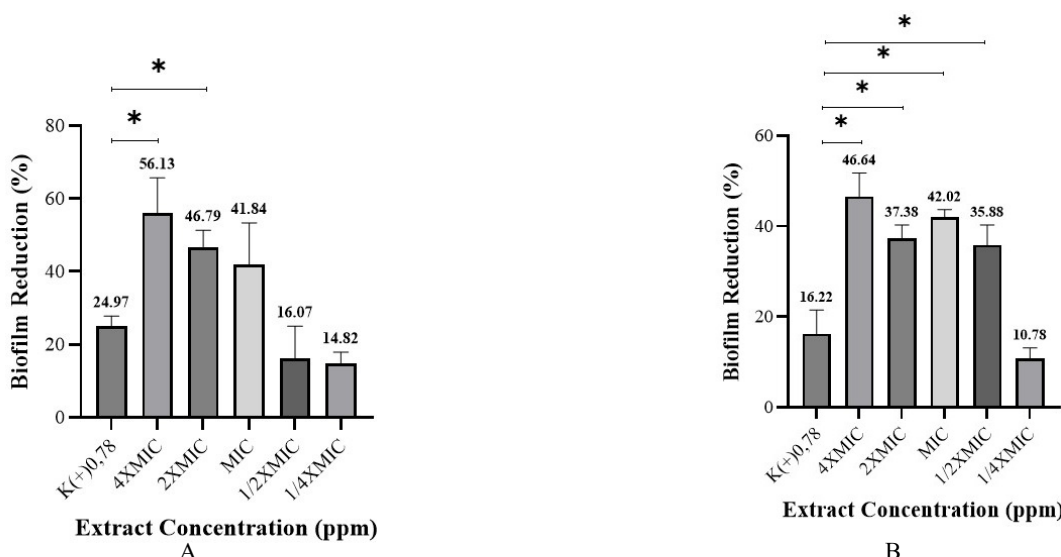


Figure 8. (A) Biofilm reduction metabolites amo.128 to *S. aureus*. (A) BRC<sub>50</sub> is 62.07 ppm. (B) Biofilm reduction metabolites amo.128 to *E. coli* with BRC<sub>50</sub> is 60.44 ppm. Statistical analysis was performed using one-way ANOVA, followed by Tukey's post hoc test with a significance level of p-value of <0.05

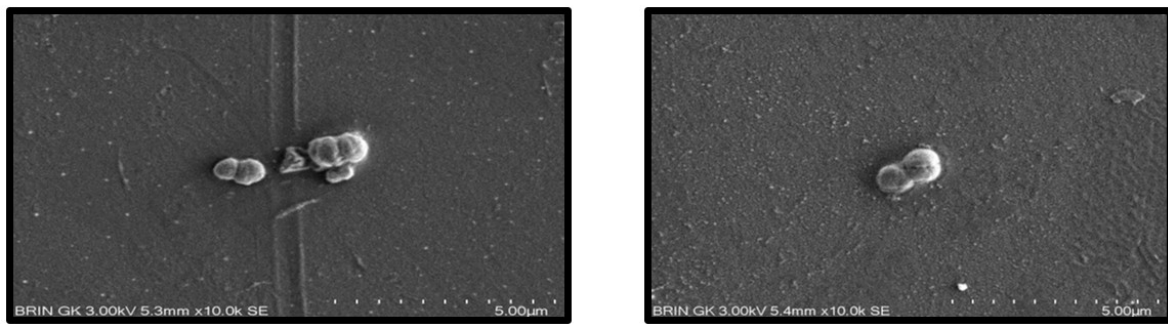


Figure 9. Scanning electron microscope (10.000X) of *S. aureus* biofilm after treatment ampicillin at (A) MIC 0.78 ppm and (B) MBC 13 ppm

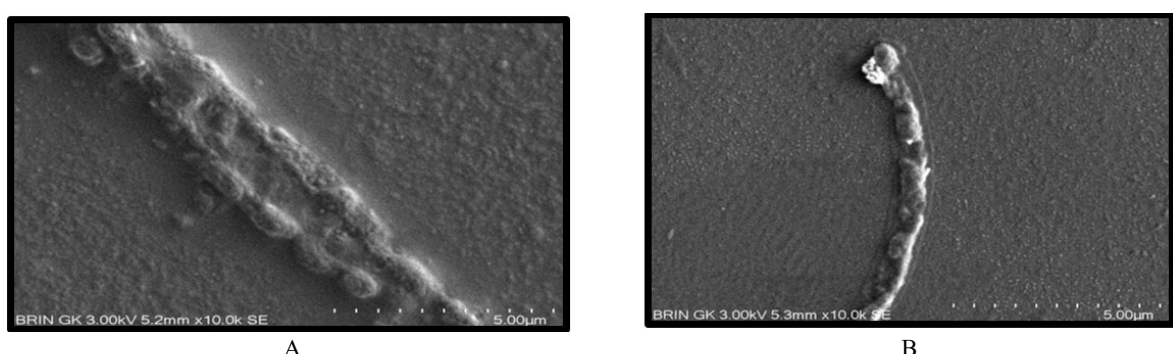


Figure 10. Scanning electron microscope (10.000X) of *E. coli* biofilm after treatment ampicillin at (A) MIC 0.78 ppm and (B) MBC 13 ppm

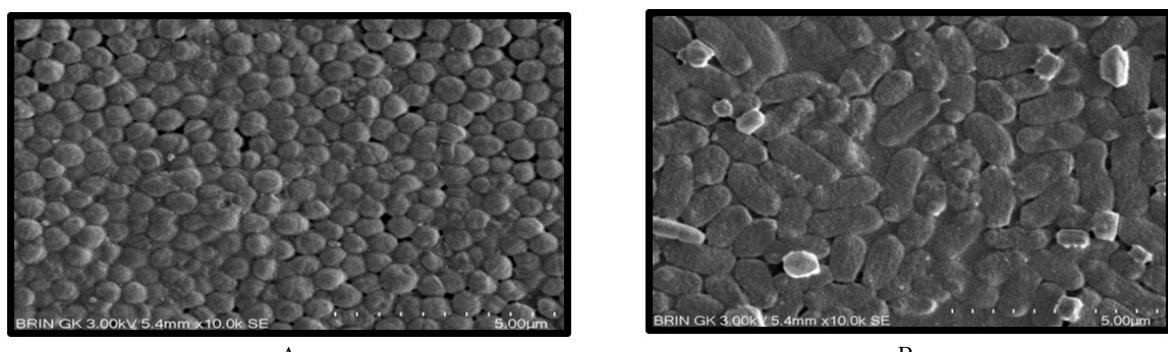


Figure 11. Scanning Electron Microscope (10.000X) of (A) *S. aureus* biofilm and (B) *E. coli* biofilm as growth control

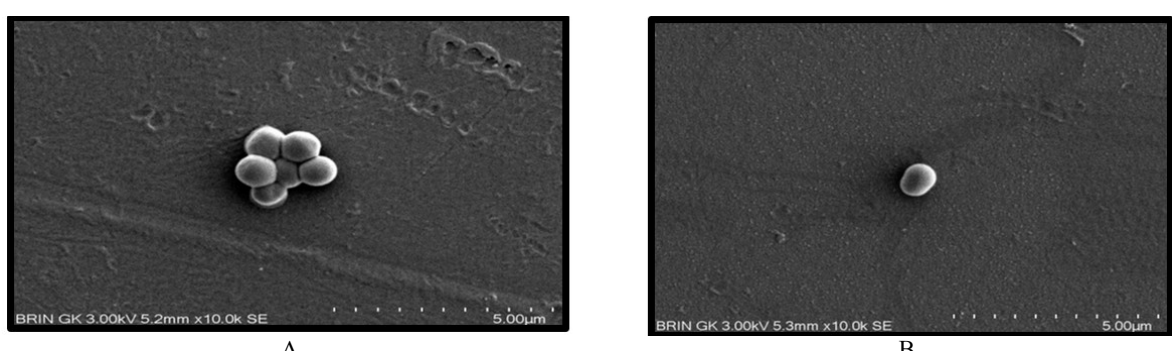


Figure 12. Scanning electron microscope (10.000X) of *S. aureus* biofilm after treatment metabolites amo.128 at (A) MIC 25 ppm and (B) MBC 50 ppm

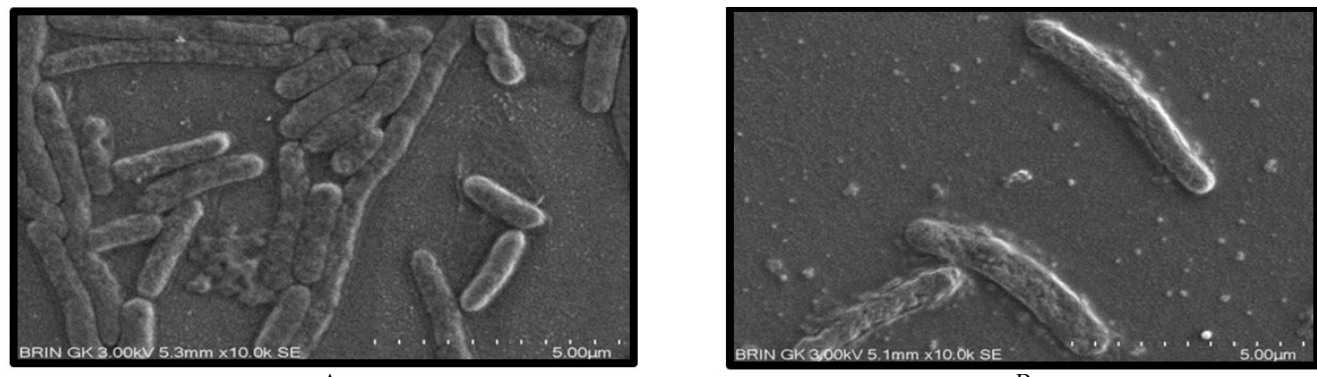


Figure 13. Scanning electron microscope (10.000X) of *E. coli* biofilm after treatment metabolites amo.128 at (A) MIC 100 ppm and (B) MBC 200 ppm

### 3.7. Binding Affinity and Ligan-Receptor Interaction

A total of five selected compounds from the amo.128 metabolites were used in docking stimulation using AutoDock Vina. Specific binding affinity (kcal/mol) was used to determine the docking pose, and the lowest free energy was considered the best conformation. One of the 5 ligands that have the highest potential binding affinity to the active site of the protein modeled in 3D was the cFP ligand, with an affinity of -10.0 kcal/mol and -4.2, as shown in Table 2 and Figure 14.

### 4. Discussion

Fermentation was used to obtain secondary metabolites with antibacterial and antibiofilm activity. Then, secondary metabolites were extracted using an ethyl acetate solvent. This solvent was used because it has advantages, including attracting most secondary metabolites (alkaloids, phenols, terpenoids, etc.), good stability, and easy evaporation. The extract was taken by dissolving it in absolute methanol and drying it again in a concentrator machine. The yield of ethyl acetate extract was  $\pm 0.0124\%$ .

Figure 1 shows actinomycete amo.128 has colonies of varying sizes, a grey color, and a sandy surface. Meanwhile, in Figure 2, actinomycetes amo.128 is a unicellular organism with gram staining, and hyphae are visible under a microscope. Actinomycetes are prokaryotes that have cell walls. They are saprophytic because they can utilize a variety of substrates, both terrestrial and aquatic. Morphologically, this group resembles fungi because it has hyphae and spores (Pepper *et al.* 2015; Setyati *et al.* 2021). Using Gram staining, the amo.128 isolate appears to be a unicellular gram-positive bacterium with a purple color that still exists. Its hyphae are septate and

Table 2. Binding affinity values for amo.128 metabolite compounds

Metabolite compounds	Affinity (kcal/mol)	
	4LGW (RMSD: 0.908)	4G4K (RMSD: 1.286)
Native Ligan	-3.4	-0.5
N-acetyltyramine	-7.2	-3.9
cyclo(phenylalanyl-prolyl)/cFP	-10.0	-4.2
3-(propane-2-yl)-octahydropyrrolo[1,2-a]pyrazine-1,4-dione	-8.0	-4.0
3-[(4-hydroxyphenyl)methyl]-octahydropyrrolo[1,2-a]pyrazine-1,4-dione	-9.5	-4.6
4-methoxycinnamic acid	-7.1	-3.9

branched. From 50X magnification, the amo.128 isolate was visible to have mycelia and spores. Actinomycetes have spores, filamentous hyphae, and cell walls thick with peptidoglycan and high in G+C (57-75%) (Setyati *et al.* 2021). This peptidoglycan binds to a crystal violet color, so the color remains purple and does not disappear when washed with alcohol. The macroscopic form of the amo.128 isolate grown on ISP2 agar media looks like a fungus. The amo.128 isolate appears to have irregular colonies, smooth convexity, uneven margins, a white color, a sandy surface, and a yellowish from the backside. Based on the characteristics above, the amo.128 isolate was close to the characteristics of the genus *Streptomyces* (Del Carratore *et al.* 2022).

Figure 3 illustrates the gel electrophoresis process. Agarose gel electrophoresis analysis of 16S rRNA genes amplified from amo.128 isolates. PCR-amplified products were run on 1% agarose gel. The results showed a single gene with a length of about 1500 bp, indicating amplification of the 16S gene. Molecular identification using the 16S rRNA gene is often used in

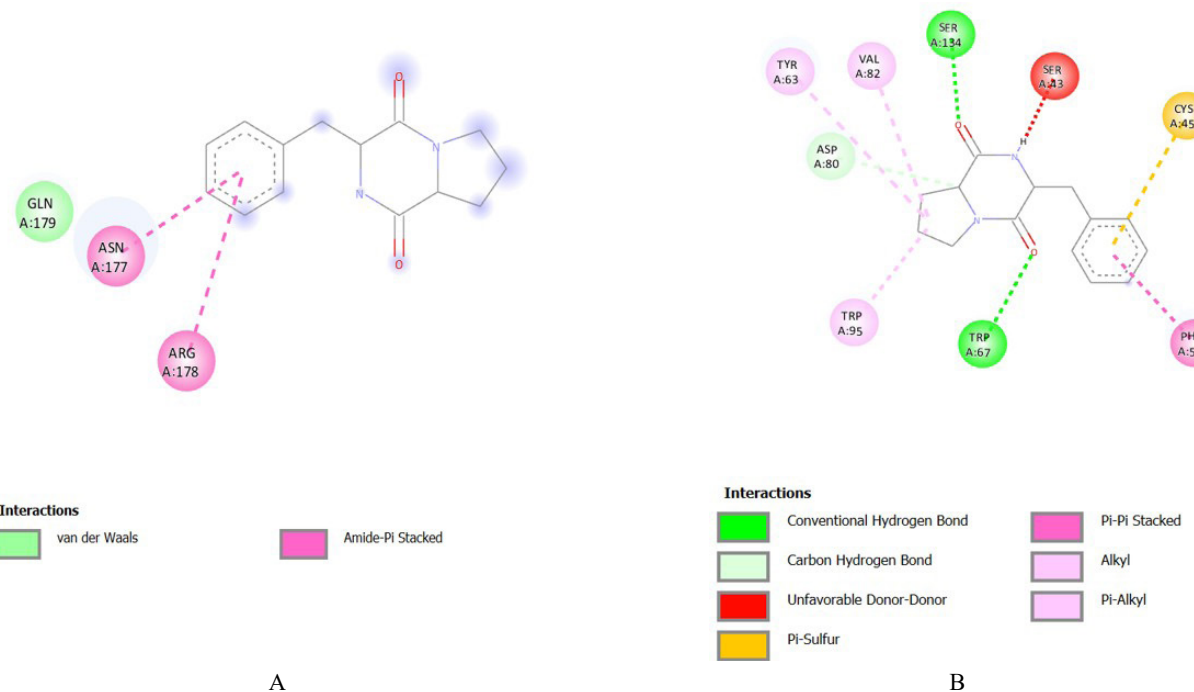


Figure 14. 2D and 3D visualization of cFP and protein target (A) *AgrA* and (B) *SdIA*

identifying bacteria. The 16S rRNA gene is universally present in every type of bacteria, and there are conserved regions that show high similarity within one species. In actinomycetes, if the 16S gene sequence homology is less than 99%, it can be said to be a different species (Komaki 2023). There are also variable regions that can provide diversity so that they can differentiate between species. Another advantage of using the 16S rRNA gene target is that several microorganisms are difficult to identify physiologically and biochemically.

However, there is also a weakness with this method. Even though they are identified as the same, their physiological and morphological properties may be different (Nurkanto & Agusta 2015). On the other hand, it is very difficult to distinguish organisms that have a very high sequence similarity. The results of BLAST sequencing on NCBI with the 16S ribosomal RNA database showed that several types of microorganisms were 100% like the isolate sequence. Reference sequences from several microorganisms are downloaded in FASTA files, which will be used to determine the phylogenetic tree using MEGA11. Phylogenetic trees illustrate the relationships between several types of actinomycetes. The amo.128 has a 100% similarity in the 16S rRNA gene sequence to *Streptomyces parvus* strain NBRC 14599 (Figure 4).

FTIR and HRMS were used to identify metabolite compounds in isolate extract. Based on the absorbance in

Figure 15, there is vibration absorption at wave numbers 3340.17  $\text{cm}^{-1}$ , 3255.92  $\text{cm}^{-1}$ , indicating the presence of -OH and N-H stretch groups, in the region of 2924.66  $\text{cm}^{-1}$  and 2854.66  $\text{cm}^{-1}$ , indicating the presence of C-H stretch. Meanwhile, in the fingerprint region of 1000 to 2000, there is a wave number of 1738.69  $\text{cm}^{-1}$  which indicates the presence of C=O stretch, absorption at 1646.40  $\text{cm}^{-1}$ , 1626.33  $\text{cm}^{-1}$  and 1582.79  $\text{cm}^{-1}$  indicate aromatic C=C, absorption at 1488.42 to 1402.55  $\text{cm}^{-1}$  indicate S=O stretch and absorption at 1192.01  $\text{cm}^{-1}$  and 1094.69  $\text{cm}^{-1}$  indicate phenolic (Bradley 2015).

The chemical compounds were identified based on m/z best fit. The relative abundance of N-acetyltyramine, cyclophenylalanylprolyl, 3-(propan-2-yl) octahydropyrrolo[1,2a] pyrazine-1,4-dione and 3-[(4-hydroxyphenyl) methyl]-octahydropyrrolo[1,2a] pyrazine-1,4-dione is 16.66%, 7.97%, 4.02%, 2.43%, respectively. N-acetyltyramine is a type of secondary amine. Phenylalanylprolyl/cFP and pyrrolo-pyrazine compounds also contain amine and carbonyl groups. N-acetyltyramine is part of the tyramine class, in which an acetyl group substitutes the amino group. This metabolite is commonly found in the sea and has quorum-sensing inhibitor activity. N-acetyltyramine is an alkaloid that is often associated with anti-free radical, antithrombotic, antitumor, and quorum-sensing inhibitor activities (Reina et al. 2019). Cyclophenylalanylprolyl/cFP has activity as a membrane integrity antagonist and antibiotic-like

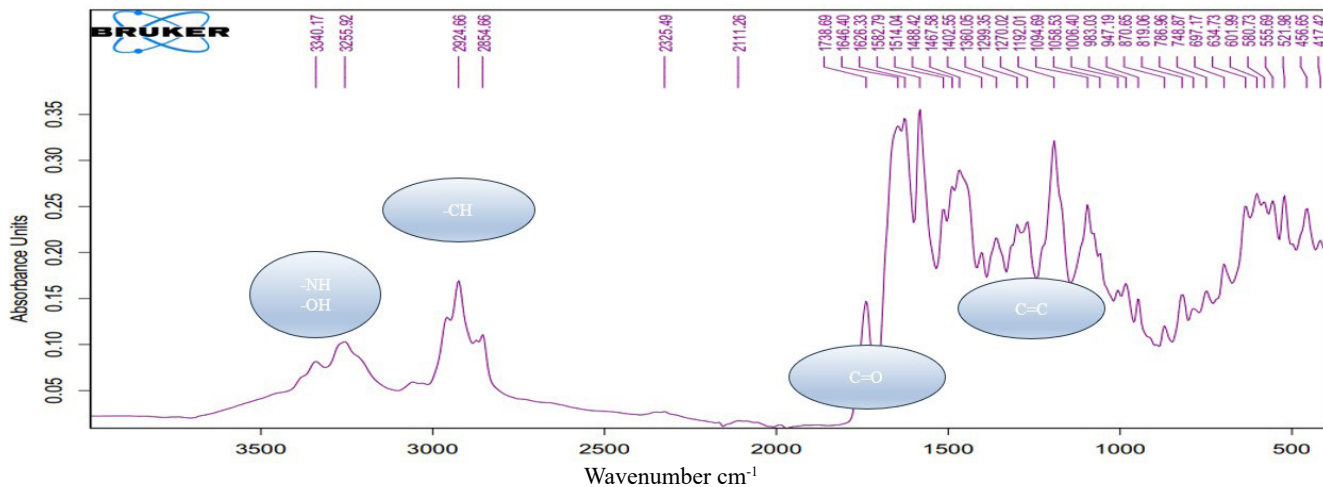


Figure 15. FTIR spectra of metabolites actinomycete amo.128

glycopeptide. cFP can inhibit biofilms by reducing the formation of biofilms and damaging the structure of biofilms up to the transcription level of PIA genes (icaA, icaC, icaD) and quorum sensing genes (*agrA*, *agrC*, *agrD*, *geh*, and *hla*) (Li *et al.* 2022). Propane-2-yl)-octahydronnoro[1,2a] pyrazine-1,4-dione and 3-[(4-hydroxyphenyl)methyl]-octahydronnoro[1,2a] pyrazine-1,4-dione is pyrrole-pyrazine derivative that has a variety of activities such as antibacterial, anti-inflammatory, antipyretic, analgesic, antioxidant, anticancer, and kinase inhibition (Chen *et al.* 2023). Kinase inhibition plays a role in the QS inhibitor mechanism, which is related to the formation of biofilms (Alenazi *et al.* 2024). The compound 4-methoxy cinnamic acid/MCA contains 2 carbonyl groups, namely ketones and carboxylates. These compounds not only have antibacterial activity but also anti-quorum sensing activity (Li *et al.* 2024).

The antibacterial activity was assessed using two test bacteria: *S. aureus*, representing Gram-positive strains, and *E. coli*, representing Gram-negative strains. This test uses a liquid microdilution method that can be used for qualitative and quantitative tests. This method just needs a little material and a sample ( $\mu\text{L}$ ) to get the value of the MIC (Schumacher *et al.* 2018). Minimum inhibitory concentration (MIC) is the smallest concentration of an antimicrobial that can inhibit the growth of test bacteria after being incubated for 24 hours. The MIC value varies for each microbe, depending on its sensitivity. MIC using microdilution was seen from the turbidity of the media in a 96-well plate after 24 hours of incubation. Antibacterial activity was measured based on the concentration series and tested using test microbes with a turbidity of  $1 \times 10^7$  cfu/ml. The bacterial turbidity was adjusted using Mc.

Farland's standard. The clear well at plate 96 was set as the MIC value against the test microbe. Isolate has a MIC value of 25 ppm for *S. aureus* and 100 ppm for *E. coli*. That value shows that metabolite isolate is more sensitive to gram-positive bacteria (Figure 5). The MBC was obtained by streaking the bacteria on MHA and incubating them for 24 hours at a temperature of 37°C. MBC is the lowest concentration of an antibacterial that can kill 99.9% of test microbes in agar media. The MBC value of metabolite extract was 50 ppm in *S. aureus* and 200 ppm in *E. coli* (Figure 6).

Figure 7 explains the inhibition of the extract concentration series. There was no significant difference in activity at a concentration of 100-400 ppm, but it was significantly different from the ampicillin control ( $p < 0.05$ ). The  $\text{MIC}_{50}$  value was calculated using linear regression, and the values for *S. aureus* were 28.48, and for *E. coli* were 49.38. Both MIC and  $\text{MIC}_{50}$  metabolites of isolate extract are more active against Gram-positive bacteria.

The antibacterial mechanism can occur in several ways, such as inhibiting protein-peptidoglycan synthesis, inhibiting enzyme metabolism, and inhibiting DNA replication, which ultimately results in the death of the bacteria. N-acetyltyramine/NAT may have antibacterial activity by degrading amino acid and peptide sequences, thereby inhibiting peptidoglycan synthesis by the transpeptidase enzyme (Cochrane & Lohans 2020; Wang & Xie 2020). Cyclophenylalanylprolyl is a cyclic dipeptide compound often found in the metabolites of microorganisms. Peptide compounds are thought to have antibacterial activity by binding to ribosomes and inhibiting the translation process so that bacterial protein synthesis is disrupted (Polikanov *et al.* 2018; Starr *et al.*

2022). The mechanism of action of the pyrrole-pyrazine derivative compounds in biological systems is still unclear. The pyrrolo [1,2-a] pyrazine derivative tends to have antibacterial, antifungal, and antiviral activity, while the 5H-pyrrolo [2,3-b] pyrazine derivative tends to act as a kinase inhibitor (Dehnavi *et al.* 2021). Meanwhile, the compound 4-methoxy cinnamic acid is thought to also have antibacterial activity by inhibiting the formation of cell walls and cell membranes, similar to the mechanism in fungi (Wang *et al.* 2023).

The biofilm detection uses 1% crystal violet staining, where the formed biofilm was dyed using 1% crystal violet. The crystal violet will bind negatively charged molecules like polysaccharides (Nuryastuti 2014). After washed by PBS, the remaining biofilm was dissolved using ethanol and measured at a wavelength of 595 nm. Figure 8 explains biofilm reduction due to the administration of extracts at concentrations of 1/4 MIC to 4x MIC. In *S. aureus*, concentrations of 2-4xMIC gave a significant difference with the ampicillin control, while in *E. coli*, a significant difference was at 1/2-4x MIC ( $p<0.05$ ). The  $BC_{50}$  value was determined using linear regression, and the value for *S. aureus* was 62.07, and *E. coli* was 60.44 ppm. This reduction was likely due to the compounds in the extract that could damage components in the biofilm, namely polysaccharides, lipids, or proteins.

Observation of biofilms using SEM was carried out by growing microbes in coverslips and treating them with isolate extract at MIC and MBC concentrations. It was also carried out on ampicillin as a control. Using SEM to see the ampicillin controls, almost no biofilm or bacterial growth was detected (Figure 9 and 10). Meanwhile, bacterial control was observed to have spherical and stem growth of *S. aureus* and *E. coli* (Figure 11). For isolate extract at the concentration of MIC and MBC *E. coli*, there was little damage, while in *S. aureus* microbes, there was almost no biofilm growth (Figure 12 and 13).

The mechanism as an anti-biofilm agent is from several compounds in the metabolites of amo.128 ethyl acetate extracts, including N-acetyltyramine/NAT. This compound is a derivative of the amino acid tyrosine. It can interfere with biofilm formation by inhibiting attachment and inhibiting quorum sensing, which is related to the process of biofilm formation (Reina *et al.* 2019). The cyclophenylalanylprolyl compound, which is a cyclic dipeptide compound, has activity in inhibiting the initial attachment of bacteria, directly damaging biofilms, and inhibiting transcription of genes related to quorum sensing (Li *et al.* 2022). The compound 3-(propane-2-yl)-octahydropyrrolo[1,2-a] pyrazine-1,4-dione and

3-[(4-hydroxyphenylmethyl]-octahydropyrrolo[1,2-a] pyrazine-1,4-dione is a pyrrole-pyrazine group compound which is a derivative of the pyrazine group. Many derivatives of pyrazine compounds have antibacterial and anticancer activity as well as biofilm eradication agents (Chen *et al.* 2023). The mechanism for inhibiting biofilm formation is thought to be through inhibition of quorum sensing as well as by 4-methoxy cinnamic compounds (Li *et al.* 2024).

Molecular docking is performed to predict ligand and protein binding. Molecular docking begins with validation, which is important to ensure that the docking results are accurate in accordance with the initial ligand position. In the above test, the RMSD values for 4LGW and 4G4K are 0.908 and 1.286. The docking interaction involves amino acids from the target protein and the test ligand (Figure 15). Docking involves several bonds, such as van der Waals bonds and hydrogen bonds. The van der Waals bond is a bond formed from the attraction between molecules, which arises from the polarization of molecules into dipoles. Hydrogen bonds occur between H atoms that are attracted to more electronegative atoms, such as O, F, or N atoms. Hydrogen bonds are stronger than van der Waals bonds.

N-acetyltyramine, cyclophenylalanylprolyl, 3-(propane-2-yl) octahydropyrrolo[1,2a] pyrazine-1,4-dione and 3-[(4-hydroxyphenyl) methyl]-octahydropyrrolo[1,2a] pyrazine-1,4-dione, and 4-methoxycinnamic acid have binding affinity to target proteins. Based on molecular binding affinity (Table 2), the compounds in the isolated extract have the potential to be developed as a quorum-sensing inhibitor. One of the compounds is cyclophenylalanylprolyl/cFP. cFP, which inhibits *SdiA* and *AgrA* with binding affinities of -10.0 and -4.2, had better affinity compared to that of native ligands, i.e. -3.4 and -0.5.

Quorum sensing is essential for microbes. Quorum sensing is responsible for expressing biofilm-forming genes (Dimitrova *et al.* 2023). Based on molecular docking Figure 15), several compounds in the extract/metabolite amo.128 have an affinity for target proteins related to quorum sensing, namely *AgrA* and *SdiA*. The affinity for *SdiA* is higher considering that there are more interactions involving amino acid residues such as serine, tryptophan, tyrosine, valine, asparagine, cysteine, and phenylalanine, while in *AgrA*, the interactions are only with the amino acids glycine, asparagine, and arginine. The suppressor of division inhibitor (*SdiA*) is a homologous LuxR protein of the dimer-shaped QS receptor that receives signals from autoinducers. Bacteria produce these autoinducers

to control virulence factors, one of which is the formation of biofilms (Culler *et al.* 2018). *AgrA* is a transcription factor that controls the operon *agr* and is responsible for biofilm formation. In gram-positive bacteria, AIP is synthesized by the *AgrD* precursor and pumped out of the cell with the help of *AgrB*. Once it reaches the quorum limit, it will enter the cell again with the help of *AgrC*. When it binds to *AgrC*, it phosphorylates *AgrA* so that *AgrA* is active and binds to the promoter of the target gene. *AgrA* binds to DNA in the P2 and P3 sections, and the transcription process can be done (Tan *et al.* 2018).

## Acknowledgements

The authors would like to appreciate the National Research and Innovation Agency, BRIN, especially the Biotechnology Laboratory, Serpong, which has provided actinomycetes isolate as research material and the PRTPP microbiology laboratory in Playen Gunungkidul in supporting material testing.

## References

Alenazi, N.A., Aleanizy, F.S., Alqahtani, F.Y., Aldossari, A.A., Alanazi, M.M., Alfaraj, R., 2024. Anti-quorum sensing activity of poly-amidoamine dendrimer generation 5 dendrimer loaded kinase inhibitor peptide against methicillin-resistant *Staphylococcus aureus*. *Saudi Pharmaceutical Journal*. 32, 101932. <https://doi.org/10.1016/j.jsp.2023.101932>

Asnani, A., Ryandini, D., Suwandri, 2016. Screening of marine *Actinomycetes* from Segara Anakan for natural pigment and hydrolytic activities. *IOP Conf. Ser.: Mater. Sci. Eng.* 107, 012056. <https://doi.org/10.1088/1757-899X/107/1/012056>

Bradley, M., 2015. FTIR basic organic functional group reference chart. Available at: <https://www.thermofisher.com/blog/materials/a-gift-for-you-an-ftir-basic-organic-functional-group-reference-chart/>. [Date accessed: 16 October 2024]

Chen, G.Q., Guo, H.Y., Quan, Z.S., Shen, Q.K., Li, X., Luan, T., 2023. Natural products–pyrazine hybrids: a review of developments in medicinal chemistry. *Molecules*. 28, 7440. <https://doi.org/10.3390/molecules28217440>

Cochrane, S.A., Lohans, C.T., 2020. Breaking down the cell wall: strategies for antibiotic discovery targeting bacterial transpeptidases. *European Journal of Medicinal Chemistry*. 194, 112262. <https://doi.org/10.1016/j.ejmech.2020.112262>

Culler, H., Couto, S., Higa, J., Ruiz, R., Yang, M., Bueris, V., Franzolin, M., Sircili, M., 2018. Role of *SdiA* on biofilm formation by atypical enteropathogenic *Escherichia coli*. *Genes*. 9, 253. <https://doi.org/10.3390/genes9050253>

Dehnavi, F., Alizadeh, S.R., Ebrahimzadeh, M.A., 2021. Pyrrolopyrazine derivatives: synthetic approaches and biological activities. *Med Chem Res.* 30, 1981–2006. <https://doi.org/10.1007/s00044-021-02792-9>

Dimitrova, P.D., Damyanova, T., Paunova-Krasteva, T., 2023. *Chromobacterium violaceum*: a model for evaluating the anti-quorum sensing activities of plant substances. *Scientia Pharmaceutica*. 91, 33. <https://doi.org/10.3390/sciparm91030033>

Del Carratore, F., Hanko, E.K., Breitling, R., Takano, E., 2022. Biotechnological application of *Streptomyces* for the production of clinical drugs and other bioactive molecules. *Current Opinion in Biotechnology*. 77, 102762. <https://doi.org/10.1016/j.copbio.2022.102762>

El Karkouri, A., Assou, S.A., El Hassouni, M., 2019. Isolation and screening of actinomycetes producing antimicrobial substances from an extreme *Moroccan* biotope. *PanAfrican Medical Journal*. 33, 1–9. <https://doi.org/10.11604/pamj.2019.33.329.19018>

Gach, M.W., Lazarus, G., Simadibrata, D.M., Sinto, R., Saharman, Y.R., Limato, R., Nelwan, E.J., Van Doorn, H.R., Karuniawati, A., Hamers, R.L., 2024. Antimicrobial resistance among common bacterial pathogens in Indonesia: a systematic review. *The Lancet Regional Health - Southeast Asia*. 26, 100414. <https://doi.org/10.1016/j.lansea.2024.100414>

Gunathilaka, G.A.D.K.K., Dewasmika, W.A.P.M., Sandaruwan, U.M., Neelawala, N.G.D.A.K., Madhumali, G.E.D., Dissanayake, B.N., Priyantha, M.A.R., Prasada, D.V.P., Dissanayake, D.R.A., 2024. Biofilm-forming ability, antibiotic resistance, and phylogeny of *Escherichia coli* isolated from extraintestinal infections of humans, dogs, and chickens. *Comparative Immunology, Microbiology and Infectious Diseases*. 105, 102123. <https://doi.org/10.1016/j.cimid.2023.102123>

Karygianni, L., Ren, Z., Koo, H., Thurnheer, T., 2020. Biofilm matrixome: extracellular components in structured microbial communities. *Trends in Microbiology*. 28, 668–681. <https://doi.org/10.1016/j.tim.2020.03.016>

Komaki, H., 2023. Recent progress of reclassification of the genus *Streptomyces*. *Microorganisms*. 11, 831. <https://doi.org/10.3390/microorganisms11040831>

Li, H., Li, C., Ye, Y., Cui, H., Lin, L., 2022. Inhibition mechanism of cyclo (L-Phe-L-Pro) on early stage *Staphylococcus aureus* biofilm and its application on food contact surface. *Food Bioscience*. 49, 101968. <https://doi.org/10.1016/j.fbio.2022.101968>

Li, Y., Ding, W., Yin, J., Li, X., Tian, X., Xiao, Z., Wang, F., Yin, H., 2024. 2,3-Dimethoxycinnamic acid from a marine actinomycete, a promising quorum sensing inhibitor in *Chromobacterium violaceum*. *Marine Drugs*. 22, 177. <https://doi.org/10.3390/md22040177>

Magiorakos, A.P., Srinivasan, A., Carey, R.B., Carmeli, Y., Falagas, M.E., Giske, C.G., Harbarth, S., Hindler, J.F., Kahlmeter, G., Olsson-Liljequist, B., Paterson, D.L., Rice, L.B., Stelling, J., Struelens, M.J., Vatopoulos, A., Weber, J.T., Monnet, D.L., 2012. Multidrug-resistant, extensively drug-resistant and pandrug-resistant bacteria: an international expert proposal for interim standard definitions for acquired resistance. *Clinical Microbiology and Infection*. 18, 268–281. <https://doi.org/10.1111/j.1469-0691.2011.03570.x>

Miller, T., Waturangi, D.E., Yogiara, 2022. Antibiofilm properties of bioactive compounds from *Actinomycetes* against foodborne and fish pathogens. *Scientific Reports*. 12, 18614. <https://doi.org/10.1038/s41598-022-23455-8>

Nirwati, H., Damayanti, E., Sholikhah, E.N., Mutofa, M., Widada, J., 2022. Soil-derived *Streptomyces* sp. GMR22 producing antibiofilm activity against *Candida albicans*: bioassay, untargeted LC-HRMS, and gene cluster analysis. *Helyon*. 8, e09333. <https://doi.org/10.1016/j.helyon.2022.e09333>

Nitbani, F.O., Jumina, Siswanta, D., Sholikhah, E.N., Nurohmah, B.A., 2020. An improved synthesis of 1-monoolein. *IOP Conference Series: Materials Science and Engineering*. 823, 012004. <https://doi.org/10.1088/1757-899X/823/1/012004>

Nurkanto, A., Agusta, A., 2015. Identifikasi molekular dan karakterisasi morfo-Fisiologi actinomycetes penghasil senyawa antimikroba (molecular identification and morphophysiological characterization of actinomycetes with antimicrobial properties). *Jurnal Biologi Indonesia*. 11, 195–203.

Nuryastuti, T., 2014. Current *in vitro* assay to determine bacterial biofilm formation of clinical isolates. *Journal of Thee Medical Sciences*. 46, 142–152. <https://doi.org/10.19106/JMedScie004603201406>

Pepper, I.L., Charles P Gerba, Terry J. Gentry. 2015. *Environmental Microbiology*; third edition. Academic Press.

Polikanov, Y.S., Aleksashin, N.A., Beckert, B., Wilson, D.N., 2018. The mechanisms of action of ribosome-targeting peptide antibiotics. *Frontiers in Molecular Biosciences*. 5, 48. <https://doi.org/10.3389/fmolb.2018.00048>

Pompilio, A., Scocchi, M., Mangoni, M.L., Shirooie, S., Serio, A., Karatoprak, S., Süntar, I., Khan, H., Bonaventura, G.D., 2023. Bioactive compounds: a goldmine for defining new strategies against pathogenic bacterial biofilms? *Critical Reviews in Microbiology*. 49, 117–149. <https://doi.org/10.1080/104041X.2022.2038082>

Reina, J.C., Pérez-Victoria, I., Martín, J., Llamas, I., 2019. A quorum-sensing inhibitor strain of *Vibrio alginolyticus* blocks qs-controlled phenotypes in *Chromobacterium violaceum* and *Pseudomonas aeruginosa*. *Marine Drugs*. 17, 494. <https://doi.org/10.3390/md17090494>

Sarika, K., Sampath, G., Kaveriyappan Govindarajan, R., Ameen, F., Alwakeel, S., Al Gwaiz, H.I., Raja Komuriah, T., Ravi, G., 2021. Antimicrobial and antifungal activity of soil actinomycetes isolated from coal mine sites. *Saudi Journal of Biological Sciences*. 28, 3553–3558. <https://doi.org/10.1016/j.sjbs.2021.03.029>

Sauer, K., Stoodley, P., Goeres, D.M., Hall-Stoodley, L., Burnmølle, M., Stewart, P.S., Bjarnsholt, T., 2022. The biofilm life cycle: expanding the conceptual model of biofilm formation. *Nature Reviews Microbiology*. 20, 608–620. <https://doi.org/10.1038/s41579-022-00767-0>

Schumacher, A., Vranken, T., Malhotra, A., Arts, J.J.C., Habibovic, P., 2018. *In vitro* antimicrobial susceptibility testing methods: agar dilution to 3D tissue-engineered models. *European Journal of Clinical Microbiology & Infectious Diseases*. 37, 187–208. <https://doi.org/10.1007/s10096-017-3089-2>

Setiawati, 2021. Fraksinasi dan uji aktivitas senyawa antimikroba dan antibiofilm dari aktinomisetes asli Indonesia [Thesis]. Yogyakarta, Indonesia: Gadjah Mada University.

Setyati, W.A., Pringgenies, D., Soenardjo, N., Pramesti, R., 2021. Actinomycetes of secondary metabolite producers from mangrove sediments, Central Java, Indonesia. *Veterinary World*. 2620–2624. <https://doi.org/10.14202/vetworld.2021.2620-2624>

Starr, A.M., Zabet-Moghaddam, M., San Francisco, M., 2022. Identification of a novel secreted metabolite cyclo(phenylalanyl-prolyl) from *Batrachochytrium dendrobatidis* and its effect on *Galleria mellonella*. *BMC Microbiology*. 22, 293. <https://doi.org/10.1186/s12866-022-02680-1>

Sunaryanto, R., Marwoto, B., Irawadi, T.T., Mas'ud, Z. A., Hartoto, L., 2009. Isolasi dan penapisan aktinomisetes laut penghasil antimikroba. *ILMU KELAUTAN*. 14, 98–101.

Suresh, S., Prathiksha Prabhakara Alva, Ramya Premanath, 2021. Modulation of quorum sensing-associated virulence in bacteria: carbohydrate as a key factor. *Arch Microbiol*. 203, 1881–1890.

Tan, L., Li, S.R., Jiang, B., Hu, X.M., Li, S., 2018. Therapeutic targeting of the *Staphylococcus aureus* accessory gene regulator (agr) system. *Frontiers in Microbiology*. 9, 55. <https://doi.org/10.3389/fmicb.2018.00055>

Wang, D., Wang, C., Gui, P., Liu, H., Khalaf, S.M.H., Elsayed, E.A., Wadaan, M.A.M., Hozzein, W.N., Zhu, W., 2017. Identification, bioactivity, and productivity of actinomycins from the marine-derived *Streptomyces heliomycini*. *Frontiers in Microbiology*. 8, 1147. <https://doi.org/10.3389/fmicb.2017.01147>

Wang, F., Guo, Y., Cao, Y., Zhang, C., 2022. *In vitro* antibacterial activity of palmitoleic acid isolated from filamentous microalga *Tribonema minus* against fish pathogen *Streptococcus agalactiae*. *Journal of Ocean University of China*. 21, 1615–1621. <https://doi.org/10.1007/s11802-022-5047-6>

Wang, X.J., Xie, J., 2020. Assessment of metabolic changes in *Acinetobacter johnsonii* and *Pseudomonas fluorescens* co-culture from bigeye tuna (*Thunnus obesus*) spoilage by ultrahigh-performance liquid chromatography-tandem mass spectrometry. *LWT*. 123, 109073. <https://doi.org/10.1016/j.lwt.2020.109073>

Wang, Y., Yin, M., Gu, L., Yi, W., Lin, J., Zhang, L., Wang, Q., Qi, Y., Diao, W., Chi, M., Zheng, H., Li, C., Zhao, G., 2023. The therapeutic role and mechanism of 4-Methoxycinnamic acid in fungal keratitis. *International Immunopharmacology*. 116, 109782. <https://doi.org/10.1016/j.intimp.2023.109782>

[WHO], 2017. WHO publishes list of bacteria for which new antibiotics are urgently needed. Available at: <https://www.who.int/news/item/27-02-2017-who-publishes-list-of-bacteria-for-which-new-antibiotics-are-urgently-needed>. [Date accessed: 10 October 2024]

[WHO], 2024. 10 penyebab kematian teratas. Available at: <https://www.who.int/news-room/fact-sheets/detail/the-top-10-causes-of-death>. [Date accessed: 10 September 2024]

Windarsih, A., Suratno, Warmiko, H.D., Indrianingsih, A.W., Rohman, A., Ulumuddin, Y.I., 2022. Untargeted metabolomics and proteomics approach using liquid chromatography-Orbitrap high resolution mass spectrometry to detect pork adulteration in *Pangasius hypophthalmus* meat. *Food Chemistry*. 386, 132856. <https://doi.org/10.1016/j.foodchem.2022.132856>

Wu, X., Wang, H., Xiong, J., Yang, G.X., Hu, J.F., Zhu, Q., Chen, Z., 2024. *Staphylococcus aureus* biofilm: formulation, regulatory, and emerging natural products-derived therapeutics. *Biofilm*. 7, 100175. <https://doi.org/10.1016/j.bioflm.2023.100175>